Article

Journal of Industrial Textiles

2022, Vol. 51(1S) 931S–953S

DOI: 10.1177/15280837221095204
journals.sagepub.com/home/jit
SAGE

Antibacterial easy adjustable woven compression bandage for venous leg ulcers

Abdelhamid R Aboalasaad[1,2], Muhammad Z Khan[3], Brigita K Sirková[1], Jakub Wiener[3], Irena Šlamborová[4], Amany S Khalil[2,5] and Ahmed H. Hassanin[6]

Abstract

The proposed study aims in first part to discuss the structure and behavior of short-stretch cotton woven compression bandage (WCB), and in second part the production and properties of multifunctional WCB. The bandage includes an integrated tension sensor, which causes a change in the spacing of colored threads during its deformation. The motivation of this research was to investigate the optimum techniques for compression therapy using a modified construction of cotton WCB as a tensiometer. The aim of second part is focused on an industrial product which has the easy adjustable compression and antibacterial properties. Multifunctional WCB can be produced by two methods, the first was using highly twisted warp yarns (ply twist 1800 to 2200 twist/m) and the weft yarns will be treated with silver Nano-particles (NPs). The second method was post-treatment of the WCB with three concentrations of zinc oxide NPs 1–3 % in powder form with 15 g/L acrylic binder. Silver NPs coated yarns showed a comparable antibacterial activity on both tested bacterial strains (*Escherichia coli* and *Staphylococcus aureus*) using quantitative and qualitative test methods. The WCB tested samples achieved 95–99% bacteria reduction, the nanoparticles size and its distribution were confirmed by the Zetasizer Nano, the scanning electron microscopy (SEM), and the energy dispersive

[1]Department of Technologies and Structures, Technical University of Liberec, Liberec, Czechia
[2]Department of Textile Engineering, Faculty of Engineering, Mansoura University, Mansoura, Egypt
[3]Department of Material Engineering, Technical University of Liberec, Liberec, Czechia
[4]Department of Chemistry FP, Technical University of Liberec, Liberec, Czechia
[5]Department of Textile Evaluation, Technical University of Liberec, Liberec, Czechia
[6]Materials Science & Engineering Department, School of Innovative Design Engineering, Egypt-Japan University of Science and Technology (E-JUST), New Borg El-Arab City, Alexandria, Egypt

Corresponding author:
Abdelhamid R Aboalasaad, Department of Technologies and Structures, Technical University of Liberec, Studentská 1402/2, Liberec 46117, Czechia.
Email: eabdo6@gmail.com

X-ray spectroscopy (EDXS). The practical bandage pressure by PicoPress showed significant deviations compared with theoretical pressure calculated by Laplace's equation ranges ±0.68 to ±15.64% especially at the highest extension levels.

Keywords
Woven compression bandage, extension levels, picopress pressure, Laplace's equation, antibacterial activity

Introduction

Compression bandage (CB): it is possible generally to divide it into two main categories of these medical components; namely, knitted and woven compression bandages (WCBs). The knitted CB is usually in tubular form, but it is practically different than the compression socks (hosiery),[1] whereas the WCBs have vast variety of types and techniques.

Medical CBs are designed to meet both the safety and the comfort of patients or athletics. In hot environments or at high activity levels, evaporation of sweat becomes an important avenue of body heat loss and fabrics must allow water vapor to escape on time to maintain the relative humidity between the skin and the first layer of clothing about 50%.[2,3] There are two classes of bandages in the market (normal and smart bandages): The simple or normal bandages, their price is cheap, their structure is simple and based on the plain weave.[4] The second class is smart CBs which have sensors to give the user direct reading of the exerted pressure on the part of the body during any activity, but it is so much costly compared to the first category, see Figure 1.[5]

Venous ulceration is the most common type of leg ulcers and a significant clinical problem. Chronic leg ulcers affect approximately 1% of the population and 3% of people over 65 years of age in the developed countries. The majority of leg ulcers are due to venous diseases.[6–8] Compression therapy by medical compression structures can be achieved using short- or medium- or long-stretch techniques at optimum stretch ranges (<70%) or (70–140%) or (>140%) respectively, which represents the extensibility level according to the standard focused on medical compression hosiery ENV 12718:2001.[9] As for the WCB, the practical stretch of a bandage on the human leg to achieve a sub-bandage pressure of 40 mmHg in the Gaiter area at circumference of 23 cm could be classified to short-stretch at 20–50% extension or long-stretch at 50–120%.[10,11]

Short-stretch CB such as 100% cotton and two-component compression system are mainly used for venous leg ulcers and edema. With a short-stretch CB, the muscle contraction causes an intermittent narrowing of the veins, a reduction of venous reflux, and thus an improvement in the venous pump function when the patient is walking. Long-stretch CB is suitable for uncomplicated varicose veins or athletic performance, such cases require medium pressure (30–40 mmHg).[12] In order to design effective compression bandages, researchers have attempted to describe the interface pressure applied by these bandages using mathematical models.[13–15] Few studies have been focused on the

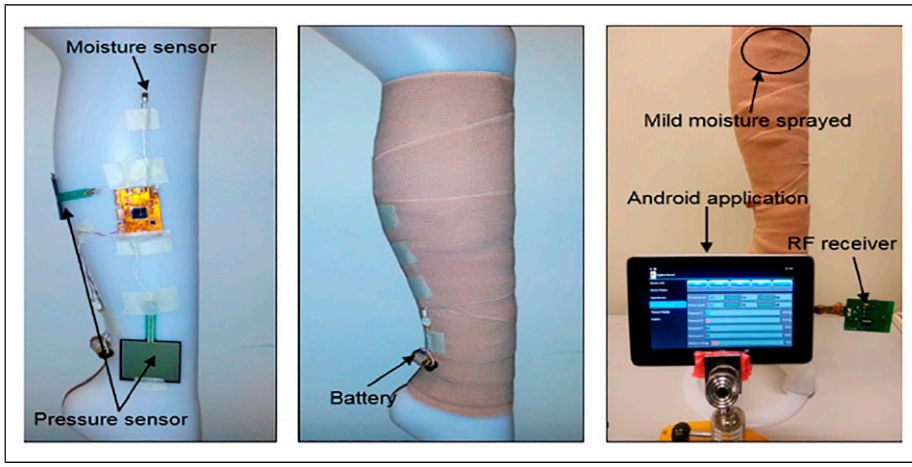

Figure 1. Smart CBs with sensor.[5]

optimization and best combinations of CBs for venous leg ulcers, edema healing, and prevention of recurrence. Most of patients depend on specialist practitioners or traditional experience. Compression therapy limits the flow of diseased surface veins, increases the flow through deeper veins, and reduces swelling. Patients who are compliant with compression therapy have significantly improved ulcer healing rate and decreased rate of recurrence. Compression is thought to either correct or improve venous hypertension, mainly owing to an improvement of the venous pump and lymphatic drainage. Compression also improves the blood flow velocity through deep and superficial veins.[16] There are three methods for producing compression bandages to achieve the optimum stretch and elasticity. First method is using highly twisted warp yarns (such as 100% cotton), the optimum elastic recovery of this CB can be achieved by adjusting the hot water treatment without tension.[4,17] The second method is using elastomeric filament (elastane or rubber) with cotton or viscose or polyamide to produce long-stretch CB. The third method is using two polymeric yarns which have different melting point by steaming and heat setting.

In clinical practice, bandages are applied in the form of overlapping layers which results in multiple layers of fabric that overlay a particular point of the surface of the limb.[18] For example, CB applied with spiral 50% overlap technique will overlay the leg with two layers of bandage, CB applied with 66% overlap will result in three layers of bandage and CB applied with the figure-of-eight technique with 50% overlap will result in four layers of bandage, see Figure 2.[19–21] Compression bandaging remains a key interference in the management of venous and lymphatic diseases. This apparently simple intervention depends on the optimum selection and practical application of four complex central properties of compression bandages, namely, applied pressure, number of layers, components, and elastic properties.[10]

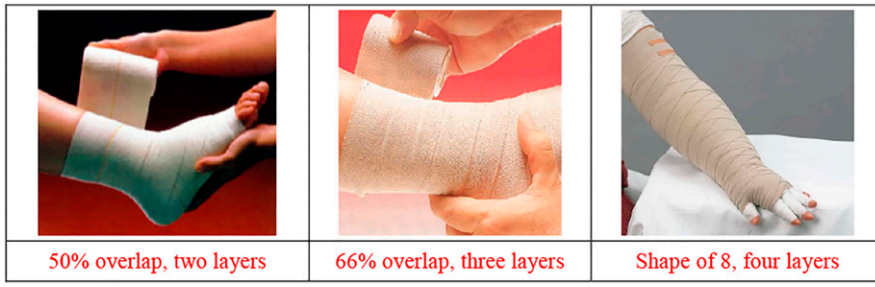

Figure 2. Three major techniques of woven compression bandages.[21]

Metal nanoparticles (MNPs), such as silver,[22,23] gold and copper have achieved special attraction because of their catalytic,[24] electronic[25] and unique optical properties[26,27] making them very attractive in the fields of particularly sensing, bio-conjugation, and surface enhancement Raman spectroscopy.[28] One of the widespread approaches to the synthesis of MNPs involves the reduction reaction of metal ions in a polymeric solution.[29,30]

The proposed study was focused on the definition of structure, then modification of construction and analysis of properties, and behavior of WCBs. The research proposed a modification of the construction of WCB made of 100% cotton yarns, where the bandage included an integrated visual tension indication that caused a color change of the bandage during its deformation. The solution was visual tensiometer in the bandage in the form of weft threads with different color from the other structure of the bandage, which became visible due to extension/stress in the bandage. For the cost saving, implementation was possible as well by applying these different weft threads through the weft insertion during weaving instead of printing or adding the colored marks after bandage production.[17]

Experimental work

Materials and samples for compression bandages

The methodology plan passed through three steps, the first was to evaluate the mechanical properties of the plied warp yarns which were used for producing 100% cotton WCB available in market. The second was to produce and analyze warp yarns at a wider range of ply twist to achieve the required elasticity of the bandage. The third was to evaluate the mechanical and antibacterial properties of the WCB, see Figure 3.[21] For the first step, plied yarns from market of 20x2 and 30x2 Tex were selected at ply twist ranges from 1850 to 2300 twist/m, as illustrated in Table 4. After evaluation of the market yarns tensile properties, the plied yarn of 20x2 Tex was selected as the optimum to give the required high extensibility and elasticity of the WCB, as demonstrated in Table 1. Therefore a new produced single yarn of 20 Tex was plied at a wider range of ply twist (600–2300 twist/m) to be used as warp yarns. The weft yarns linear density was 60 Tex for the new WCB samples, its specifications are listed in Table 2.

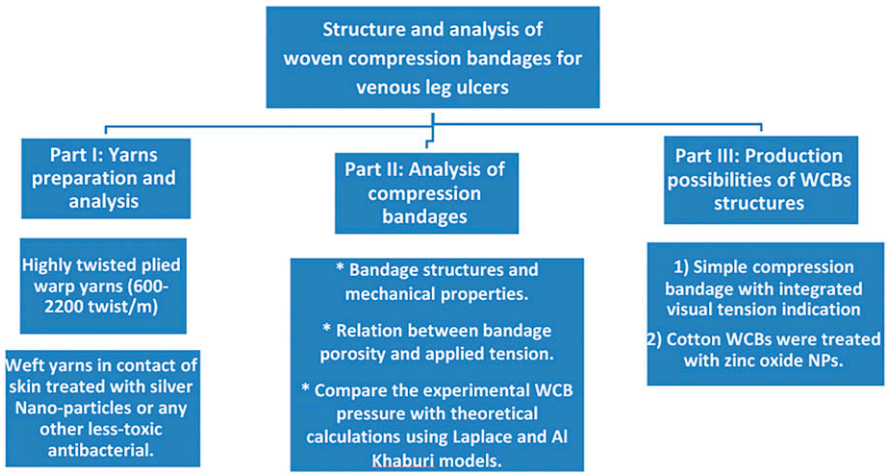

Figure 3. Overall plan of experimental work.

Table 1. Newly produced plied yarn properties, 20x2 Tex.

Twist direction					
SS-Z		SZ-Z		ZZ-S	
Ply twist, twist/m	Actual yarn count, Tex	Ply twist, twist/m	Actual yarn count, Tex	Ply twist, twist/m	Actual yarn count, Tex
606	40.03	597	40.87	602	39.63
1181	41.88	1216	42.18	1204	41.29
1761	45.78	1793	46.68	1773	48.40
2185	52.26	2168	55.45	2172	54.42

Table 2. The specifications of the woven bandage samples.

Bandage parameters	Cotton bandage, code [1], (with blue lines)	Cotton bandage, code [2]
Warp set	10 ends/cm	14 ends/cm
Weft set	15 picks/cm	18 picks/cm
Warp count	Cotton, 20x2 Tex, 1800 twist/m	Cotton, 15 x 2 Tex, 2100 twist/m and 46 Tex, 850 twist/m
Warp crimp	125%	220% and 140% respectively
Weft count	Cotton, 75 Tex, open-end yarn	Cotton, 36 Tex
Weft crimp	7.5%	11.3%
Fabric weight	210.25 g/m^2	223.83 g/m^2
Fabric thickness	1.06 mm	1.32 mm

Table 3. Samples' codes for treated cotton WCB with zinc oxide nanoparticles.

State	Sample code [1]	Sample code [2]
Untreated, standard	1- With blue color every 1 cm	2- Without colors
Treated, 1% ZnO-NPs	[1–1]	[2–1]
Treated, 2% ZnO-NPs	[1–2]	[2–2]
Treated, 3% ZnO-NPs	[1–3]	[2–3]

Colloidal form of Silver NPs was prepared using glucose as reducing agent. Poly vinyl pyrrolidone (PVP) was used as stabilizer. *Escherichia coli (E. coli)* - CCM 2024 (ATCC 9637), Gram-negative rod-shaped bacteria and *Staphylococcus aureus (S. aureus)* - CCM 2260 (ATCC 1260), Gram-positive rod-shaped bacteria were purchased from Czech collection of microorganisms, Masaryk University in Brno. Two types of WCB (fabric) samples have been treated with three concentrations of ZnO nanoparticles as follows, 1, 2, and 3% in powder form with 15 g/L binder. The samples' coding for un-treated and treated cotton WCB with zinc oxide nanoparticles (ZnO-NPs) is listed in Table 3.

Analysis of the mechanical properties of the warp yarns and WCB

The load-elongation curve of the warp yarns was measured according to the ISO 2062: 2009(E).[31] Instron 4411 tensile testing machine was used to measure the tension developed in the yarn using a gauge speed of 180 mm/min, and the device gauge length was set to 500 mm. The yarn twist per meter was measured on the TWIST LAB-2531C twist testing machine according to standard procedure CSN 80 0701. The yarn linear density was measured from a lea of one hundred meters according to CSN 80 0050. The WCB pressure was measured using the Microlab PicoPress M-700 at the ankle and mid-calf positions.[32]

The compression of living tissue using textile bandages is only estimated based on the personal experience of the bandage applicator. Based on the evaluation of deformation during the bandage application, it is possible to give the patient, nurse, or any other user accurate remarks to adjust the applied compression to the body part through the innovated colored WCB, see Figure 4. The simple bandage could be converted to a smart WCB by modifying the bandage structure such as adding the blue marks (rectangles of 2 cm x 1 cm to be squares of 2 x 2 cm^2 at 100% extension or adjusted according to the required bandage tension such as 2 x 1.5 cm^2 at 50% extension, as illustrated in Figure 5). This modification could control the bandage tension as a function of the applied extension that ranges from 50 to 100% depending on the bandage construction and the number of layers. There are three levels of bandage tension (low: 50% extension and 50% overlap, medium: 100% extension and 50% overlap, and high: 100% extension and 66% overlap).[12]

Bandage porosity is calculated by measuring the binary area fraction using high resolution camera. While subjecting the bandage samples to a constant extension, the resultant images were recorded using high resolution camera.[4]

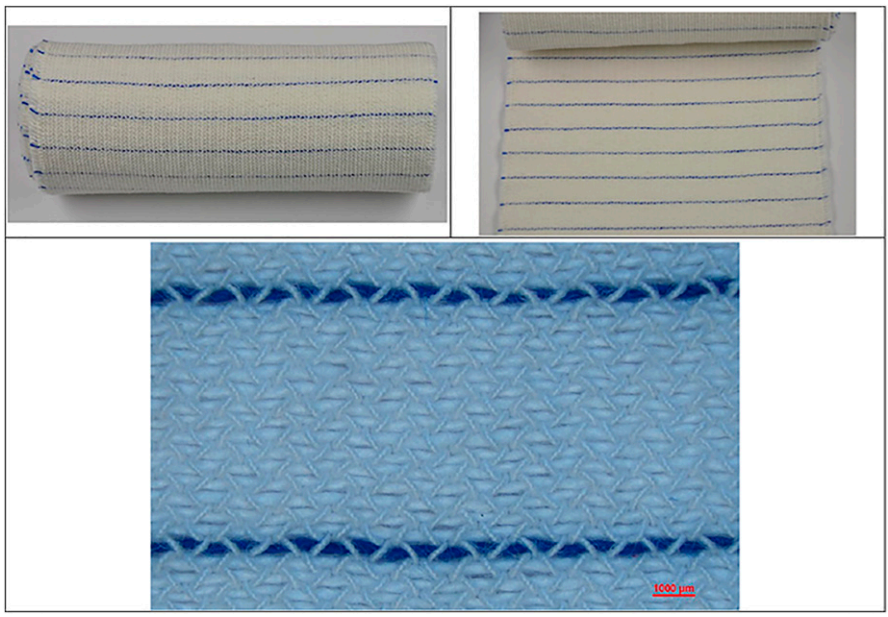

Figure 4. The innovated modification for 100% cotton WCB and its structure.

Cotton WCBs were worn one by one on real leg to test the real compression pressure at ankle and mid-calf positions in both static and walking conditions at different extension levels. Ankle and calf positions were adjusted at leg circumference of 25.6 and 38.9 cm respectively. Deviation percent was calculated according to equation (3), as the difference between measured compression using PicoPress and calculated pressure by Laplace's equations (1 & 2),[14,33] as illustrated in Figure 8. The level of pressure exerted on a medical device matches with the Laplace's equation stating that the pressure (P expressed in Pa) of a compression applied to the skin surface is directly proportional to the tension (T in N) of the compression material and number of layers, and inversely proportional to the radius of curvature (R in m) of limb surface to which it is applied and the bandage width (W in m).[34]

$$Pressure(Pascal) = \frac{Tension(N) * No.\,of\ Layers}{Radius(m) * Bandage\,width\ (m)} \tag{1}$$

$$Pressure(mmHg) = \frac{T(N) * n}{R\ (m) * W(m)} * 0.0075 \tag{2}$$

$$\text{Deviation percent}(\%) = \frac{\boldsymbol{P}_{\boldsymbol{Calculated}} - \boldsymbol{P}_{\boldsymbol{Picopress}}}{\boldsymbol{P}_{\boldsymbol{Calculated}}} x\,100 \tag{3}$$

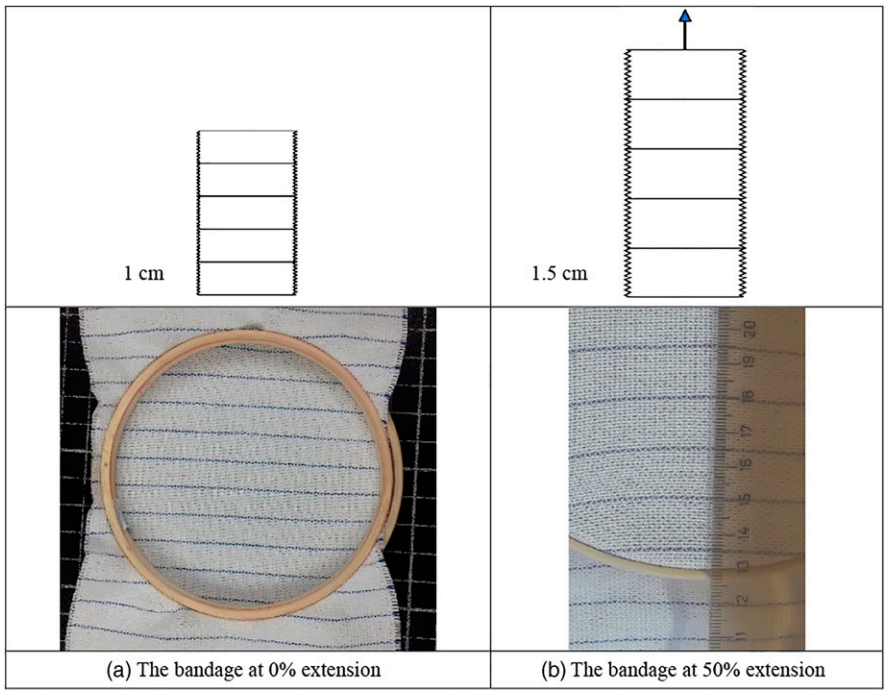

Figure 5. A colored weft repeated every 1 cm during the bandage weaving.

Antibacterial treatment and activity of the weft yarns and WCB

Preparing cotton weft yarns treated with Silver NPs. Uniform silver nanoparticles (Ag-NPs) were obtained by reduction of Silver nitrate at 70°C under atmospheric pressure. Glucose Ag-NPs were synthesized by dissolving $AgNO_3$ (157 mg) and PVP (5 g) in 100 mL of 40% (w/w) of glucose syrup. 5 mL of sodium chloride were added to the samples for complete reaction and to convert all the ionic Silver to NPs.[35] Ten samples, 200–300 m of bleached cotton yarns were winded on perforated Polypropylene bobbins, their thickness ranges from 5 to 10 mm. Five samples were immersed in glucose Ag-NPs solution for 1 min (D_1) and the other samples for 60 min (D_2). The treated samples were dried at 90°C, and then cured for 4 min at 130°C.

Silver NPs activity of treated yarns. For the tests, pathogenic bacterial strains were used for the qualitative test method (AATCC 147) and quantitative test method (AATCC 100).

A) Method AATCC 147: 1 mL of the bacterial inoculums (*E. coli and S. aureus*) at a concentration of 10^8 CFU/ml was individually inoculated onto Petri blood agar plate, the test sample was inserted into the middle of the plate. The prepared samples were cultivated in thermostat 24 h/37°C.[36] This is a qualitative method. After 24 h of incubation, the growth of bacteria under the test sample and the zone of inhibition are evaluated. The

method can be used to verify whether the active substance is released from the sample into the environment (halo zones of different sizes appear) or whether the active substance is bound in the sample and the effect is manifested only below the sample.[37]

B) Method AATCC 100: 100 µl of *E. coli* and *S. aureus* at a concentration of 10^8 CFU/ml were applied on the sample. The sample was placed in a sterile container and cultured 24 h/37°C. After 24 h, 10 mL of physiological solution was added and the sample was shaken. 1 mL of solution was removed and plated onto Petri blood agar plate. The samples were cultured for 24 h/37°C. The antibacterial activity of Ag-NPs treated cotton fabrics was quantitatively determined before and after washing using bacterial percentage reduction test, AATCC 100–2004, according to the American Association of Textile Chemists and Colorists Technical Manual 2010.[38] It is a quantitative method in which a reduction factor is evaluated, which indicates the percentage by which the concentration of inoculated bacteria has been reduced. The percentage reduction was determined as following equation (4):[39,40]

$$Reduction(\%) = \frac{(C - A)}{C} \tag{4}$$

where C and A are the colonies counted from the plate of the control and treated sample, respectively.

Coating of cotton WCBs with ZnO nanoparticles. ZnO nanoparticles at 1–3 wt% concentration in powder form and 15 g/L binder were added into distilled water and the dispersion was sonicated for 10 min using ultrasonic system (Bandelin Sonopuls HD 3200, 20 kHz, 200 W, 50% efficiency). Then, the ZnO nanoparticles dispersion was applied on the cotton WCB through a dip-pad-dry-cure method. The cotton WCB was immersed into the dispersion for 1 min, subsequently passed through a padder, dried at 100°C in a drying oven and finally cured at 150°C for 5 min to ensure that the ZnO nanoparticles adhere to the cotton WCB surface.[41]

The antibacterial tests were performed according to the following standards; AATCC 147 Test Method: 147–2012 - Assessment of Antibacterial Activity of Textile materials: Parallel Streak Method, and AATCC 100 Test Method: 100–2019 - Assessment of Antibacterial Finishes on Textile Materials.

Results and discussion

Evaluation of load-elongation curves of plied warp yarns

The evaluation of the used plied warp yarns in market for producing the WCB and the new produced yarns concluded that the warp yarn's tenacity should be greater than 16 cN/Tex and its extension should be at least 12% to produce the highly stretched 100% cotton WCB, as displayed in Table 4 & Figure 6. The twist range (1500–1800 twist/m) is required – at least – for producing high extension cotton compression bandages, whereas to achieve 100% elastic cotton compression bandage (2000–2200 twist/m) would be used. The new produced yarns have a wider range of twist and higher tenacity by average 19%.

Table 4. Commercial plied warp yarns' properties.

			Tenacity		Extension	
Nominal yarn count (Tex)	Actual yarn count (Tex)	Yarn twist (twist/m)	Average (cN/Tex)	Std. (cN/Tex)	Extension (%)	Std. (%)
20*2	42.07	1200	18.5615	0.7808	10.5424	0.6346
	45.29	1600	16.8927	0.9227	11.2619	0.6783
	49.37	1850	15.5338	0.8982	12.0127	0.6491
	51.15	2100	12.8549	0.8860	12.1918	0.6298
30*2	74.72	2200	9.8618	1.0965	15.7838	0.7483
	80.27	2300	8.5234	1.2289	15.7745	0.6144

The optimum extension level and applied load mainly depends on the final end-use of the WCB either for venous leg ulcers or athletic performance.[4] The optimum pressure for the edema recovery, medium pressure on ankle position was 35 mmHg whereas mid-calf position was 21 mmHg. There was a gradual decreasing compression starting at the ankle, then calf, to the knee as illustrated in Figures 7 and 8.

The obtained results in Figure 8 confirm that there are significant deviations when applying Laplace's equation for two and three layers bandaging ranging ±0.68 to ±15.64%. The highest deviation values were clearly significant at high extension levels 60–80%, this might be due to the compactness and high compression especially at ankle position. Moreover Jawad Al Khaburi developed this equation (5) to include the increase in limb circumference due to multilayer bandaging; this equation has decreased the deviation range to be ±0.07: ±12.55% as illustrated in the following equations[18,42]:

$$P_n = \sum_{i=1}^{n} \frac{T_i(D_i + t_i)}{0.5 * W_i * D_i^2 + W_i * t_i(D_i + t_i)} * 0.0075 \tag{5}$$

$$D_i = D + \sum_{i=1}^{n} 2t_{i-1} \tag{6}$$

Where **i** is the bandage layer, $\mathbf{t_i}$ is the extended and compressed bandage layer thickness in (m), $\mathbf{T_i}$ is the tension in (N), $\mathbf{W_i}$ is the extended bandage width in (m), **D** is the limb diameter in (m), $\mathbf{D_i}$ is the combined limb diameter and previous bandage layers thickness, and $\mathbf{P_n}$ is the pressure induced by n number of bandage layers in (mmHg).

As for the application of 100% cotton bandage on real leg, the bandage horizontal porosity has been analyzed as a function of the bandage extension level and the angle between warp and weft threads, as displayed in Figure 9.[32] Evaluation of the angle between warp and weft as well as the bandage porosity were performed on the basis of image analysis according to an internal standard IS 23–107-01/01.[43] The methodology of scanning and evaluation of the porosity of woven fabric consists in determination of the covered threshold area (displayed by red color) of woven fabric microscopic specimen in

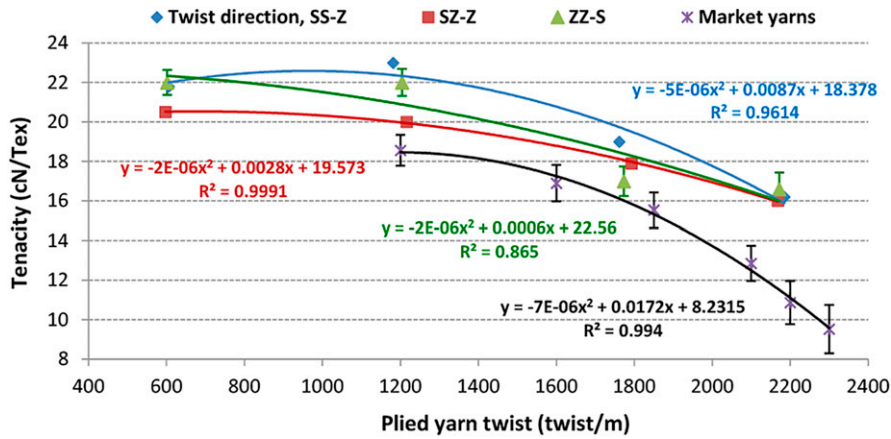

Figure 6. Effect of plying twist on yarn tenacity for new produced and market yarns.

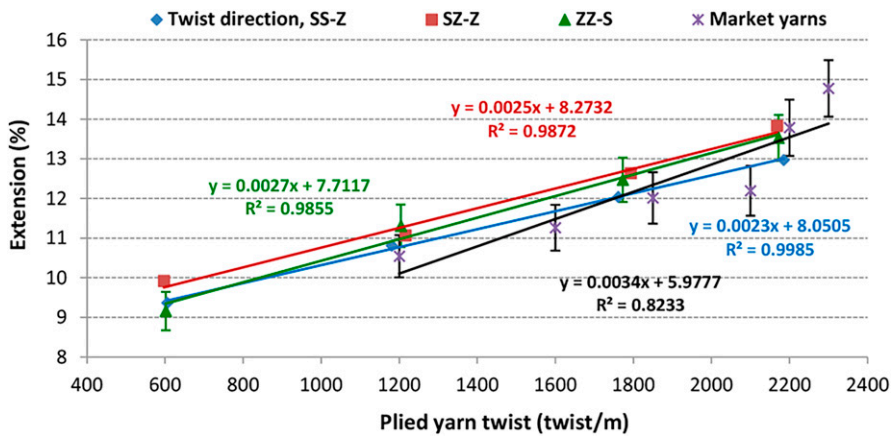

Figure 7. Effect of plied yarn twist on its extension for produced and market yarns.

transmitted light. Moreover the average value of angles and the bandage porosity are presented in Figure 9.

Silver NPs activity of treated cotton yarns

Silver nanoparticles possess a broad spectrum of antibacterial, antifungal, and antiviral properties. Silver nanoparticles have the ability to penetrate bacterial cell walls, changing the structure of cell membranes and even resulting in cell death. Their efficacy is due not only to their nanoscale size but also to their large ratio of surface area to volume. They can

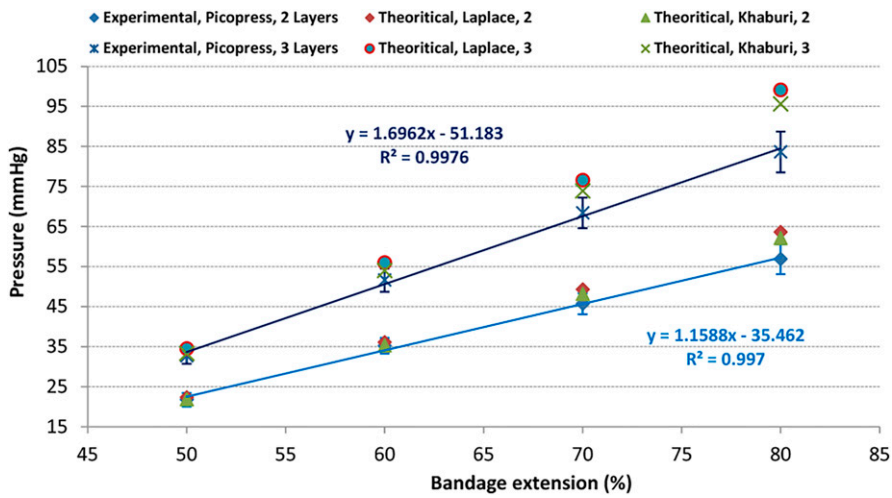

Figure 8. Measured bandage pressure by PicoPress versus calculated by Laplace's and Al-khaburi's equations at ankle position using two and three layers of cotton bandage.

increase the permeability of cell membranes, produce reactive oxygen species, and interrupt the replication of deoxyribonucleic acid by releasing silver ions.

The antibacterial actions of silver nanoparticles:

1) Disruption of the cell wall and cytoplasmic membrane: silver ions (Ag^+) released by silver nanoparticles adhere to or pass through the cell wall and cytoplasmic membrane. 2) Denaturation of ribosomes: silver ions denature ribosomes and inhibit protein synthesis. 3) Interruption of adenosine triphosphate (ATP) production: ATP production is terminated because silver ions deactivate respiratory enzyme on cytoplasmic membrane. 4) Membrane disruption by reactive oxygen species: reactive oxygen species produced by the broken electron transport chain can cause membrane disruption. 5) Interference of deoxyribonucleic acid (DNA) replication: silver and reactive oxygen species bind to deoxyribonucleic acid and prevent its replication and cell multiplication. 6) Denaturation of membrane: silver nanoparticles accumulate in the pits of cell wall and cause membrane denaturation. 7) Perforation of membrane: silver nanoparticles directly move across cytoplasmic membrane, which can release organelles from cell.

Method AATCC 147. Treated test samples (D_1 and D_2) showed comparable antibacterial activities on both tested strains (*E. coli* and *S. aureus*). The antibacterial activity of D_1 and D_2 is significantly appeared through clear inhibition zone (measured as the average thickness of inhibition zone only in one side of treated yarns) compared to the standard sample (D_0) that does not show any inhibition of bacteria strains, as illustrated in Table 5 and Figure 10.

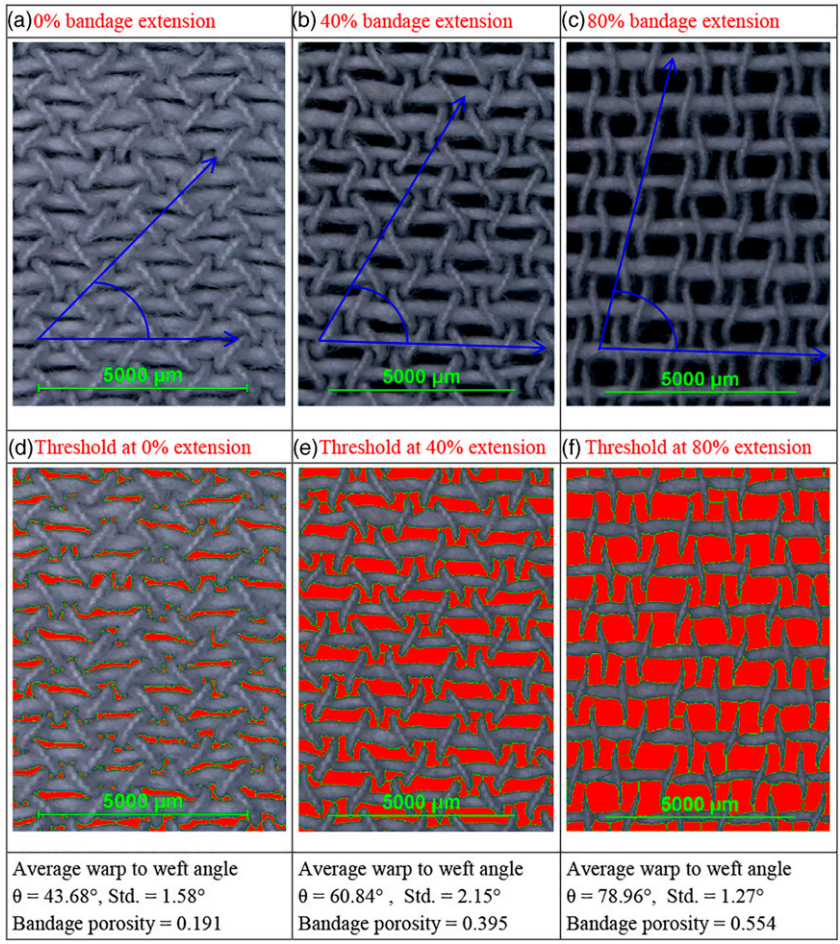

Figure 9. Effect of extension level on the horizontal porosity of cotton bandage during application on real leg.

Table 5. Inhibition zone of treated yarns according to AATCC 147.

Method ATCC147	Sample D_0 standard	Sample D_1	Sample D_2
Escherichia coli	No effect	Inhibition zone 1,44 mm	Inhibition zone 1,58 mm
Staphylococcus aureus	No effect	Inhibition zone 2,06 mm	Inhibition zone 2,01 mm

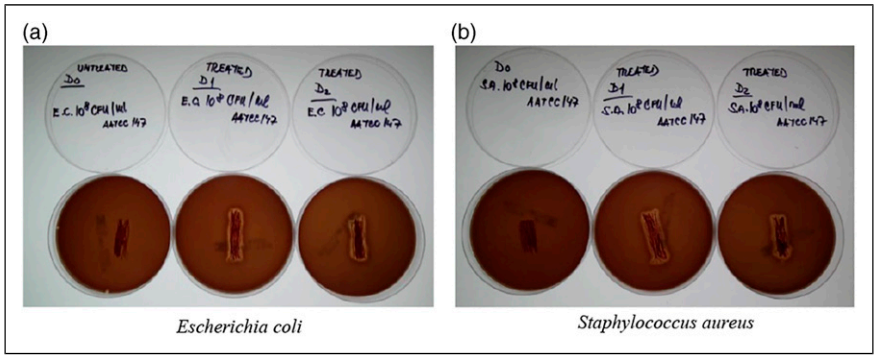

Figure 10. Inhibition zone of treated yarns against.

Method AATCC 100. The number of surviving bacterial colonies are considered and counted in this test method, see Table 6. Compact incidence means that the number of surviving bacterial colonies is not countable, as shown in Figure 11.

Scanning electron microscopy and energy dispersive X-ray of the yarns

The scanning electron microscopy of the treated and un-treated single and plied cotton yarn samples are illustrated in Figure 12 respectively. The silver NPs size and its distribution are demonstrated for the treated yarn samples. Moreover the energy dispersive X-ray mapping for the yarn samples confirmed the NPs percent in the total composition of yarn EDXS mapping, see Figure 13. It can be obviously noticed that the silver nanoparticles have been successfully synthesized in Nano-scale. Moreover, silver nanoparticle have been successfully attached to the yarn surface with sufficient homogenous distribution. Energy dispersive X-ray mapping, EDXS, are confirming the existence of silver Ag+ all over the treated yarn surfaces.

Verification of antibacterial activity of cotton WCB treated with Zinc Oxide NPs

The treated samples with three concentrations: 1%, 2%, and 3% ZnO Nanoparticles in powder form with 15 g/L binder showed positive results of antibacterial activity for both Gram-positive and Gram-negative bacteria strains, as listed in Table 7. Halo zones did not appear in the tested samples, as listed in Table 8. In samples [1–2], [1–3], [2–2] and [2–3], 100% inhibition was found under the sample in both tested bacterial strains, i.e. the treatment did not allow the growth of bacteria under the WCB sample. This enhancement is very positive for the bandages' applications as bactericidal treatment to kill the bacteria colonies.

The quantitative method showed 95–99% inhibition in all treated WCB samples on both tested bacterial strains compared to the standard samples. Moreover the higher concentrations of ZnO Nanoparticles were associated with comparable improvement of the antibacterial activity of treated samples.

Table 6. Antibacterial assessment by quantitative test according to AATCC 100.

Method ATCC100	D_0 standard	Sample D_1	Sample D_2
Escherichia coli	Compact incidence	0	0
Staphylococcus aureus	Compact incidence	1	0

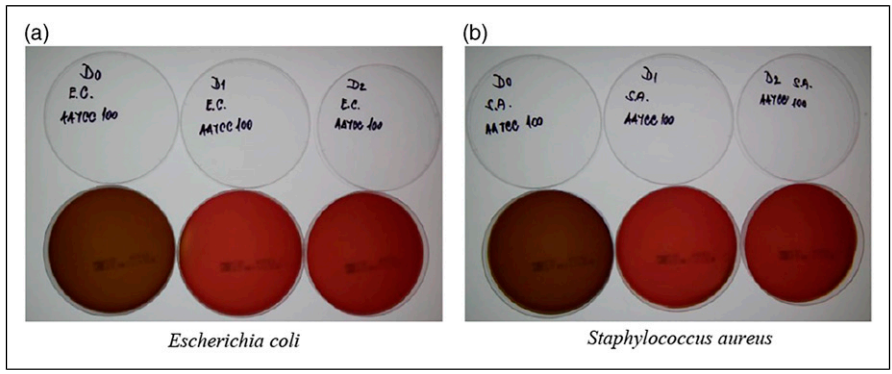

Figure 11. Surviving bacterial colonies.

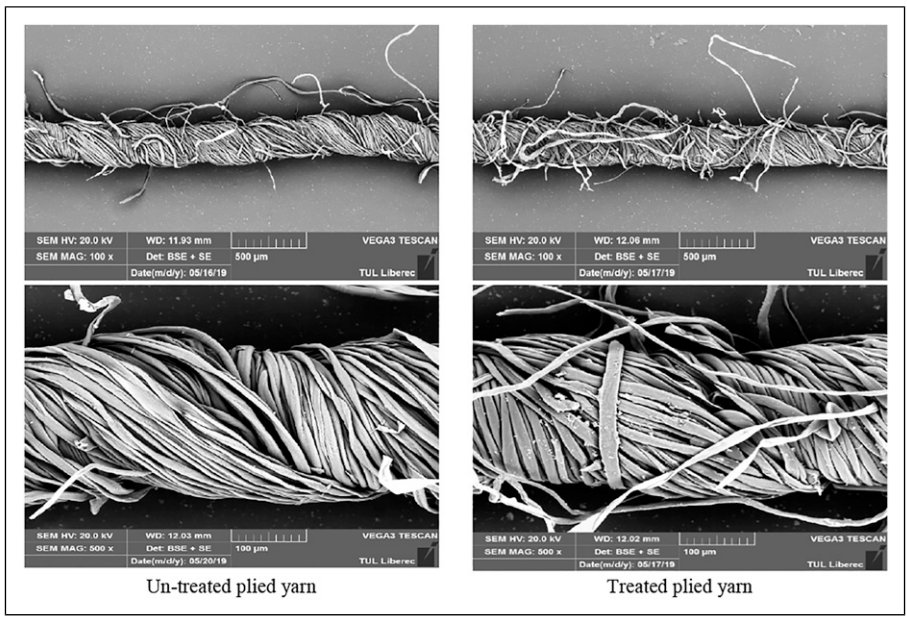

Figure 12. Scanning electron microscopy of the un-treated and treated plied yarns.

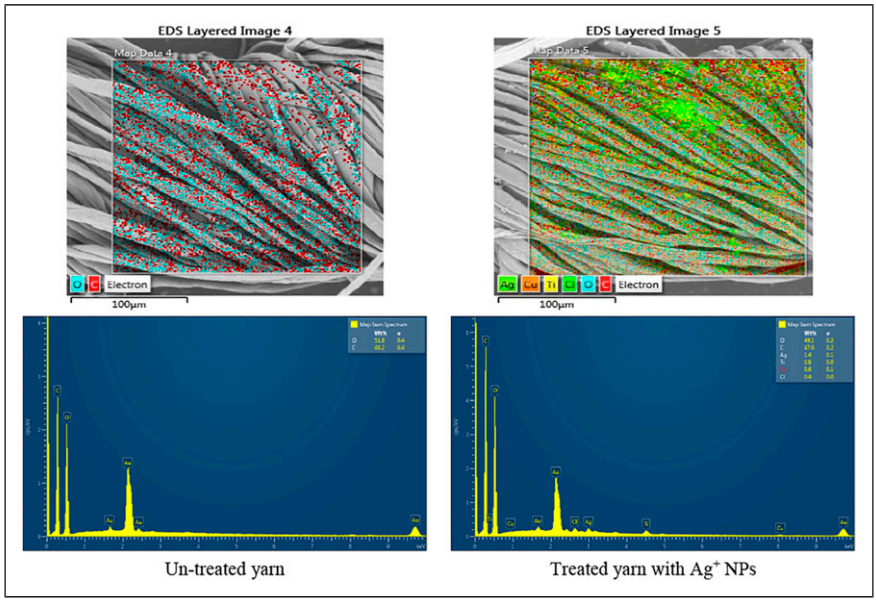

Figure 13. Energy dispersive X-ray mapping of the un-treated and treated plied yarns.

Table 7. The antibacterial activity of cotton WCB according to AATCC 147–2012.

Sample number	*Escherichia coli* inhibition zone size - mm / % inhibition below sample	*Staphylococcus aureus* inhibition zone size - mm / % inhibition below sample
Standard 1	0 mm, 0%	0 mm, 0%
[1–1]	1.13 mm, 97.5%	0.54 mm, 96%
[1–2]	2.51 mm, 100%	1.63 mm, 100%
[1–3]	3.08 mm, 100%	2.47 mm, 100%
Standard 2	0 mm, 0%	0 mm, 0%
[2–1]	0.82 mm, 96%	0.57 mm, 95.5%
[2–2]	1.93 mm, 100%	1.49 mm, 100%
[2–3]	2.71 mm, 100%	2.68 mm, 100%

The antibacterial mechanism of ZnO is mainly due to generation of reactive oxygen species such as O_2^- and OH. These species are produced due to generation of electron (e^-), and electric hole (h^+) pairs on the surface of the photocatalyst. The negative electrons (e^-) and oxygen (O_2) combine into superoxide radical ($\cdot O_2^-$), while the positive holes (h^+) and water (H_2O) produce hydroxyl radicals ($\cdot OH$). Finally, the generated hydroxyl radicals ($\cdot OH$), and superoxide radical ($\cdot O_2^-$) are responsible for the antibacterial action. Due to very high oxidative nature of reactive oxygen species, the membrane of bacteria get oxidized which cause their death. Being photocatalyst, Moreover, it has been reported

Table 8. The antibacterial activity of cotton WCB according to AATCC 100–2019.

Sample number	*Escherichia coli* % inhibition	*Staphylococcus aureus* % inhibition
Standard 1	---	---
[1–1]	96%	95%
[1–2]	98%	97.4%
[1–3]	99.5%	99%
[2–1]	96%	95%
[2–2]	97.3%	96.4%
[2–3]	98.5%	97.5%

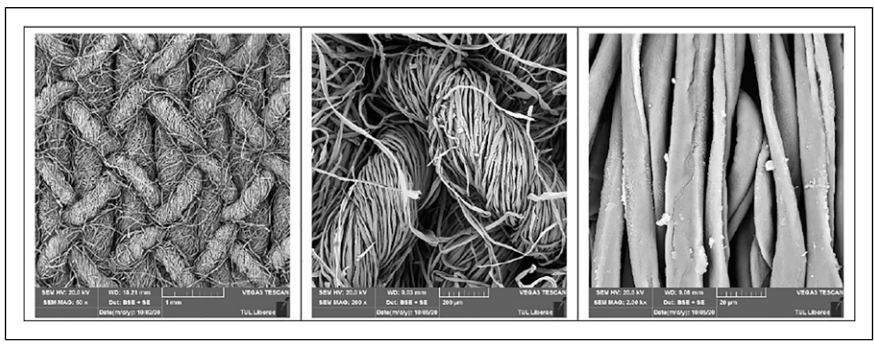

Figure 14. SEM of the un-treated cotton woven bandage, Standard 1.

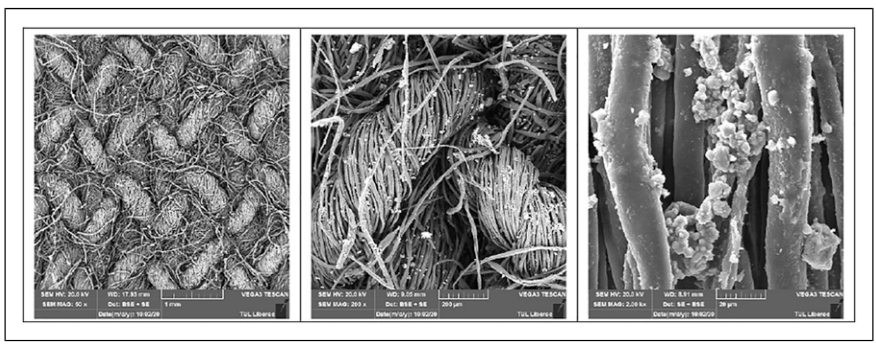

Figure 15. SEM of the treated cotton WCB with 1% zinc oxide nanoparticles, [1–1].

in previous studies that the release of Zn^{++} also plays a significant role in inhibiting the growth of bacteria.[44]

Scanning electron microscopy and energy dispersive X-ray of the bandage samples. The SEM of the un-treated and treated cotton WCB samples (Standard 1, [1–1], [1–2], [1–3]) are

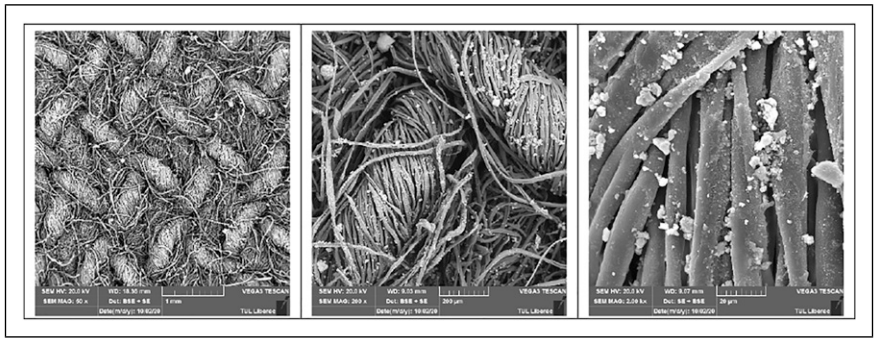

Figure 16. SEM of the treated cotton WCB with 2% zinc oxide nanoparticles, [1–2].

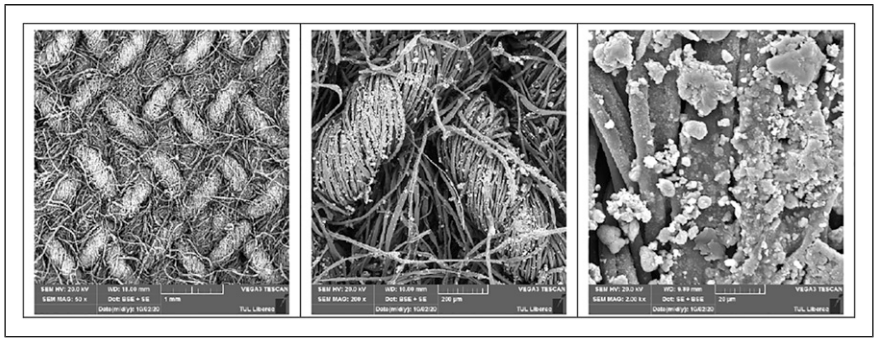

Figure 17. SEM of the treated cotton WCB with 3% zinc oxide nanoparticles, [1–3].

Table 9. Technical specification of ZnO-NPs (Bochemie, BOCH-01).

Specifcation	Results
Crystalline phase	100%
Crystallite-size of primary particles	13 ± 2 nm
Particles' size	21–23 nm
Specific surface size	90–110 g/m^2
Particle shape	Spherical

displayed in Figures 14 to 17 respectively. The zinc oxide nanoparticles' characteristics are listed in Table 9, which were then confirmed with the Zetasizer Nano.[45] Moreover the ZnO-NPs distributions are investigated for the treated bandage samples and the EDXS mapping confirmed the percent of ZnO nanoparticles' in the total composition of bandage samples, as illustrated in Figures 18 to 21 for the treated bandage samples. The optimum

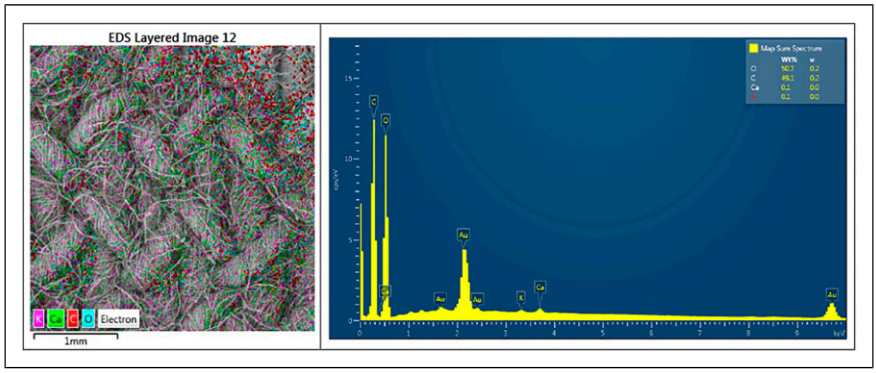

Figure 18. Energy dispersive X-ray map of the un-treated cotton WCB, Standard 1.

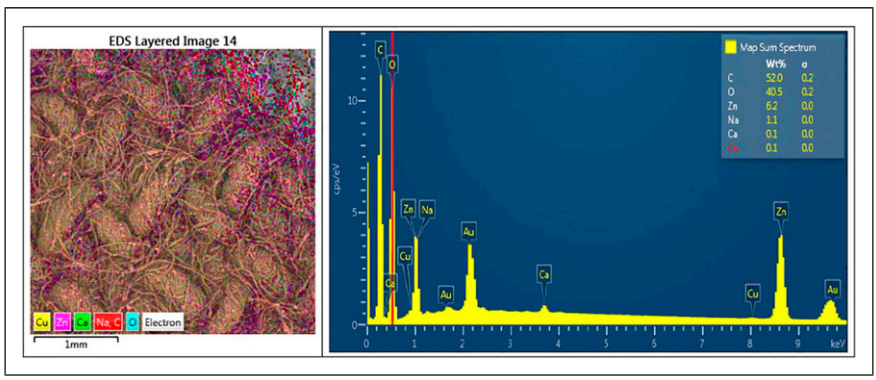

Figure 19. EDXS map of the treated cotton WCB with 1% zinc oxide nanoparticles, [1-1].

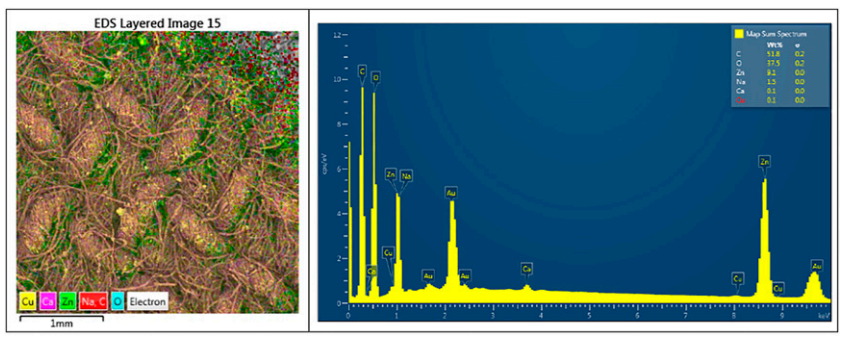

Figure 20. EDXS map of the treated cotton WCB with 2% zinc oxide nanoparticles, [1–2].

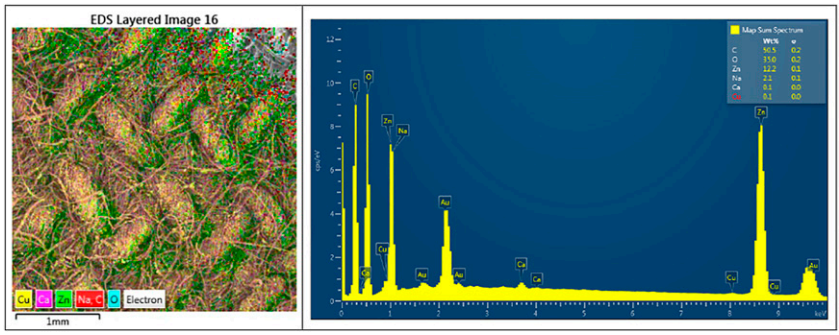

Figure 21. EDXS map of the treated cotton WCB with 3% zinc oxide nanoparticles, [1–3].

treating concentration of the ZnO NPs was 2% with higher antibacterial activity and lower agglomeration than 3%.

Conclusion and recommendation

The research aims were focused on the definition of structure, then modification of construction and analysis of mechanical and antibacterial properties of WCBs. Based on the WCB evaluation, it could be possible to create a better condition during the bandage application by a patient, nurse, or athletic user, and find a connection between the structure and applied bandage tension during static and dynamic applications. The proposed study achieved a modification of the structure and construction of 100% cotton WCB, designed an integrated tension sensor, which caused a change in the spacing of colored threads during its extension, such as rectangles of 2 cm x 1 cm could be converted to squares of 2x2 cm^2 at 100% extension. The warp yarn tenacity should be greater than 15.5 cN/Tex, and its extension should be at least 12% to produce the highly stretched 100% cotton WCB, and the optimum twist of warp yarns was ranged between 1800–2200 twist/m for producing high extension cotton WCBs. Moreover, the horizontal bandage porosity was measured as a function of applied extension and angle between warp and weft yarns.

Silver NPs coated yarn samples D_1 and D_2 showed a comparable antibacterial activity (approximately 99–99.5%) on both tested bacteria strains (*E. coli* and *S. aureus*) using both quantitative and qualitative test methods. Moreover the new produced WCB structure were treated with ZnO-NPs and had positive results of antibacterial activity (approximately 95–99%) for both Gram-positive and Gram-negative bacteria strains according to AATCC 147–2012 and AATCC 100–2019.

The coating of weft yarns with non-toxic NPs is recommended to reduce the total cost of WCB and enhance its antibacterial activity and sustainability.

Author's Note

Ahmed H. Hassanin is also affiliated to Department of Textile Engineering, Faculty of Engineering, Alexandria University, Alexandria, Egypt.

Declaration of conflicting interests

The author(s) declared no potential conflicts of interest with respect to the research, authorship, and/or publication of this article.

Funding

The author(s) disclosed receipt of the following financial support for the research, authorship, and/or publication of this article: This work was supported by the Ministry of Education, Youth and Sports of the Czech Republic and the European Union— European Structural and Investment Funds in the Frames of Operational Programme Research, Development and Education— The project Hybrid Materials for Hierarchical Structures [HyHi, Reg. No. CZ.02.1.01/0.0/0.0/16_019/0000843] and the project "Textile structures combining virus protection and comfort" (Viratex, Reg. no. CZ.01.1.02/0.0/0.0/20_321/0024467).

ORCID iDs

Abdelhamid R Aboalasaad https://orcid.org/0000-0001-8889-8203
Muhammad Z Khan https://orcid.org/0000-0001-7173-6101
Brigita K Sirková https://orcid.org/0000-0002-0675-3658
Amany S Khalil https://orcid.org/0000-0001-5021-3870

References

1. Lohmann-rauscher. Adhesive-bandages, tubular Bandage, https://www.walmart.com/browse/health/adhesive-bandages/lohmann-rauscher/976760_2571007_3742624/YnJhbmQ6TG9obWFubiiAmIFJhdXNjaGVy, (2021).
2. Huang J. Review of heat and water vapor transfer through multilayer fabrics. *Text Res J* 2016; 86: 325–336.
3. Aboalasaad ARR, Skenderi Z, Brigita Kolčavová S, et al. Analysis of factors affecting thermal comfort properties of woven compression bandages. *Autex Res J* 2020; 20: 178–185.
4. Aboalasaad ARR and Sirková BK. Analysis and prediction of woven compression bandages properties. *J Text Inst* 2019; 110: 1085–1091.
5. Mehmood N, Hariz A, Templeton S, et al. An improved flexible telemetry system to autonomously monitor sub-bandage pressure and wound moisture. *Sensors (Switzerland)* 2014; 14: 21770–21790.
6. Marola S, Ferrarese A, Solej M, et al. Management of venous ulcers: State of the art. *Int J Surg* 2016; 33: S132–S134.
7. Agale SV. Chronic leg ulcers: Epidemiology, aetiopathogenesis, and management. *Ulcers*, Epub ahead of print 2013. DOI: 10.1155/2013/413604.
8. Fletcher J, Moffatt C, Partsch H, et al. Principles of compression in venous disease. *Wounds Int* 2013: 1–21.
9. Kumar B, Das A and Alagirusamy R. Analysis of sub-bandage pressure of compression bandages during exercise. *J Tissue Viability* 2012; 21: 115–124.
10. Partsch H, Clark M, Mosti G, et al. Classification of compression bandages: Practical aspects. *Dermatol Surg* 2008; 34: 600–609.

11. Meara OS, Cullum N, Ea N, et al. Compression for venous leg ulcers (Review). *Cochrane Database Syst Rev*; 11, Epub ahead of print 2012. DOI: 10.1002/14651858.CD000265.pub3. www.cochranelibrary.com.
12. Aboalasaad ARR, Sirková BK, Bílá P, et al. Comparative study of long- and short-stretch woven compression bandages. *Autex Res J*, Epub ahead of print 2020. DOI: 10.2478/aut-2020-0035.
13. Halfaoui R and Chemani B. New approach to predict pressure produced by elastic textile in the therepeutic treatment of venous leg. *J Fundam Appl Sci* 2016; 8: 297.
14. Al Khaburi J, Dehghani-Sanij AA, Nelson EA, et al. Effect of bandage thickness on interface pressure applied by compression bandages. *Med Eng Phys* 2012; 34: 378–385.
15. Schuren J and Mohr K. The efficacy of Laplace's equation in calculating bandage pressure in venous leg ulcers. *Wounds UK* 2008; 4: 38–47.
16. Erickson CA, Lanza DJ, Karp DL, et al. Healing of venous ulcers in an ambulatory care program: The roles of chronic venous insufficiency and patient compliance. *J Vasc Surg* 1995; 22: 629–636.
17. Aboalasaad ARR, Sirková BK and Eldeeb M. Influence of woven bandage composition on its elasticity and durability. *J Text Inst* 2021; 0: 1–11.
18. Khaburi J Al, Dehghani-sanij AA, Nelson EA, et al. The effect of multi-layer bandage on the interface pressure applied by compression bandages. *World Acad Sci Eng Technol Int J Mech Aerospace, Ind Mechatron Manuf Eng* 2011; 5: 1169–1174.
19. Keller A, Müller ML, Calow T, et al. Bandage pressure measurement and training: Simple interventions to improve efficacy in compression bandaging. *Int Wound J* 2009; 6: 324–330.
20. Beharková N and Soldánová D. Basics of Nursing Practices and Interventions, https://is.muni.cz/do/rect/el/estud/lf/js19/osetrovatelske_postupy/web/pages_en/05-kompresivni_terapie.html (2019).
21. Aboalasaad ARR and Sirková BK. Structure and Analysis of Woven Compression Bandages for Venous Leg Ulcers, http://webdev.ft.tul.cz/document/3254 (2021).
22. Emam HE, Mowafi S, Mashaly HM, et al. Production of antibacterial colored viscose fibers using in situ prepared spherical Ag nanoparticles. *Carbohydr Polym* 2014; 110: 148–155.
23. Bankura KP, Maity D, Mollick MMR, et al. Synthesis, characterization and antimicrobial activity of dextran stabilized silver nanoparticles in aqueous medium. *Carbohydr Polym* 2012; 89: 1159–1165.
24. Africa S, Unit EM and Africa S. Redox catalytic property of gold nanoclusters : evidence of an electron-relay effect. *Appl Phys A* 2005; 801: 797–801.
25. Kamat P V. Photophysical, photochemical and photocatalytical aspects of metal nanoparticles. *J Phys Chem B* 2002; 106: 7729–7744.
26. Liz-Marzán LM. Tailoring surface plasmons through the morphology and assembly of metal nanoparticles. *Langmuir* 2006: 32–41.
27. Hebeish AA, El-Rafie MH, Abdel-Mohdy FA, et al. Carboxymethyl cellulose for green synthesis and stabilization of silver nanoparticles. *Carbohydr Polym* 2010; 82: 933–941.
28. Shipway AN, Lahav M and Willner I. Nanostructured gold colloid electrodes. *Adv Mater* 2000; 12: 993–998.
29. El-Rafie MH, Ahmed HB and Zahran MK. Facile precursor for synthesis of silver nanoparticles using alkali treated maize starch. *Int Sch Res Not* 2014; 2014: 1–12.

30. Emam HE and El-Bisi MK. Merely Ag nanoparticles using different cellulose fibers as removable reductant. *Cellulose* 2014; 21: 4219–4230.
31. Standard I. ISO. (2009). E. 2062. Textiles – Yarns from packages – Determination of single-end breaking force and elongation at break using constant rate of extension (CRE) tester. *ICS 59080*.
32. Aboalasaad ARR, Sirková BK and Ahmad Z. Influence of tensile stress on woven compression bandage structure and porosity. *Autex Res J* 2020; 20: 263–273.
33. Chemani B and Halfaoui R. Influence of pressure from compression textile bands: Their uses in the treatment of venous human leg ulcers. *Int J Phys Sci* 2014; 9: 146–153.
34. Rimaud D, Convert R and Calmels P. In vivo measurement of compression bandage interface pressures: The first study. *Ann Phys Rehabil Med* 2014; 57: 394–408.
35. kheybari S, Samadi N, Hosseini SV, et al. Synthesis and antimicrobial effects of silver nanoparticles produced by chemical reduction method. *DARU J Pharm Sci* 2010; 18: 168–172.
36. Ali A, Baheti V, Militky J, et al. Copper coated multifunctional cotton fabrics. *J Ind Text* 2018; 48: 448–464.
37. Alshabanah LA, Hagar M, Al-Mutabagani LA, et al. Hybrid nanofibrous membranes as a promising functional layer for personal protection equipment: Manufacturing and antiviral/antibacterial assessments. *Polymers*; 13, Epub ahead of print 1 June 2021. DOI: 10.3390/polym13111776.
38. Teli MD and Sheikh J. Modified bamboo rayon-copper nanoparticle composites as antibacterial textiles. *Int J Biol Macromol* 2013; 61: 302–307.
39. Ashraf M, Champagne P, Perwuelz A, et al. Photocatalytic solution discoloration and self-cleaning by polyester fabric functionalized with ZnO nanorods. *J Ind Text* 2015; 44: 884–898.
40. Alshabanah LA, Hagar M, Al-Mutabagani LA, et al. Biodegradable nanofibrous membranes for medical and personal protection applications: Manufacturing, anti-COVID-19 and anti-multidrug resistant bacteria evaluation. *Materials*; 14, Epub ahead of print 2021. DOI: 10.3390/ma14143862.
41. Khan MZ, Baheti V, Ashraf M, et al. Development of UV protective, superhydrophobic and antibacterial textiles using ZnO and TiO2 nanoparticles. *Fibers Polym* 2018; 19: 1647–1654.
42. Chassagne F, Molimard J, Convert R, et al. Numerical model reduction for the prediction of interface pressure applied by compression bandages on the lower leg. *IEEE Trans Biomed Eng* 2018; 65: 449–457.
43. Technická univerzita v Liberci. Internal Standards Method, https://facultystaff.richmond.edu/~cstevens/301/IS_General.html (2004).
44. Ashraf M, Dumont F, Campagne C, et al. Development of antibacterial polyester fabric by growth of ZnO nanorods. *J Eng Fiber Fabr* 2014; 9: 15–22.
45. BOCHEMIE a.s. Vive nano zinc oxide. 2021; 7534490.